

Design of Suspension Components to Determine Reliability under Racing Conditions

Fabian Fuentes Martinez¹, Albert Miyer Suarez Castrillon² and Sir-Alexci Suarez Castrillon³

^{1,2} Faculty of Engineering and Architecture. University of Pamplona, Colombia.

³ Engineering Faculty, University Francisco of Paula Santander Ocaña, Colombia.

Abstract

This article contains the design of the suspension components made to a competition car, by means of computer simulation according to the calculations made for the control arms and the projection of the support area in the connection struts, as well as the geometry of the control arms. The purpose is to determine through simulation and design of the components the most appropriate possible configuration for the manufacture of the parts of the car, where the results have the characteristics and dimensions that meet the standard, for this purpose Catia is used as a computer package, obtaining 3D representations and analyzing the materials with which they will be finally manufactured.

Keywords: Car component design, Nascar, Competition car suspension, Catia, endurance simulation.

1. INTRODUCTION

The design and construction of car bodies involves the review of several factors where the type of materials is growing in importance, if previously metallic materials or new alloys were used as a constant, today some such as polymers are being incorporated due to their advantages in design, cost and low weight [1], [2], they can also be reusable thanks to recycling which helps to significantly improve the environment [3], making it possible to manufacture new products. The main problem with polymers is the time they take to degrade, reaching up to 100 years [4], [5]. Carbon fiber is also displacing materials such as aluminum or steel, among its advantages are its mechanical strength, fatigue resistance, impact resistance, among others. That is why it has become one of the most requested materials for the construction of car bodies [6]. The first carbon fiber cars were designed for Formula 1 by the McLaren team and after several years its use intensified by large automobile construction companies [7], even if the parts cannot be built entirely with this material, it can be used as an alternative to reinforce them, since it has been used in construction [8].

The design of components used in the automotive company is focused on the casting of molds, these must be built according to the technical specifications of each part to be manufactured, the assistance systems for a reliable and safe driving is focused on adding anti-lock braking systems, airbags, seat belts, among others. The systems not only allow greater safety, but also focus on passenger comfort, component life and testing in different weather or terrain conditions [9]. At first glance the car chassis is one of the most checked and tested parts in safety tests, where

they must withstand shocks, vibrations and hard braking, in addition to centrifugal forces in curves. The test simulation of the chassis can be compared with polymer and steel materials supporting the same loads, this test process is performed with the simulation of computer packages such as Ansys, with which the numerical results are validated before the manufacturing and assembly process [10]-[12].

Racing competitions force to improve all automotive manufacturing processes, which over time are incorporated into the automotive industry that is why the design of components is essential if you want to have a better performance in a competition. Hours and hours of research are applied to the design and manufacture of all components of the competition car by simulating each of the parts in different situations. This research presents the design of components for a Nascar car, using computer simulation, and taking into account the material with which it will be manufactured, designing and simulating the suspension that supports the weight and friction and the compression force. The mechanical properties are also reviewed. All models are developed in 3D using CATIA software, in this way all components are selected. Nascar has 3 divisions, where the Monster Energy Cup Series division is the star category, and generally the tracks where it competes have an oval design [13].

2. METHOD

In permanent mold casting, molten metal is poured into a permanent metal mold simply by gravity, low pressure or centrifugal pressure. Castings of the same alloy and shape produced with a permanent mold have a finer grain structure and greater strength than castings made in a sand mold.

For the manufacture of the components that make up the system, the permanent mold die casting process was selected because it produces parts with excellent dimensional characteristics, the manufacturing speed is high and thus spare parts can be obtained quickly when needed. For the upper and lower control arms the process is very well adapted, and the geometry that was conceived is not so complex, once the part is finished the computerized machining technique is used to rectify the hole of the connection point and for the threaded holes that contain the ends for the insertion of the spherical ball joints. As for the main structure of the central module of the system and the stub axle, a preform of the basic geometry is obtained and then computer machining is used to obtain the final geometry (cavities, threaded holes). For the fabrication of the connecting

pin, computer machining or conventional turning can be used since its geometry is simple.

When the car has understeer, it is difficult to corner and tends to go straight to the outside of the curve, losing the line. To get the car to enter the corner correctly, the driver has to lift his foot off the throttle while cornering, slowing the car down. This is a condition that can be overcome during a race by adjusting factors such as tire air pressure, spring stiffness and chassis weight distribution. The car can understeer in the 3 phases of the corner, which refer to entering the corner, during the corner or through the corner and exiting the corner. The shock absorbers used to complete the suspension are of the German brand KONI suspension, the model selected is the 3012 series (3012-516318D) as it allows independent adjustment of the system sections in rebound and extension, therefore they are easy to adapt to this type of car. According to the definition of the suspension travel which is in the range of ± 2 in the selected shock absorber contains a total travel of 5 in so it meets what is required. After calculating the roll rates and spring rates to be used, we proceed to determine the relative movement between the components, which is a geometric concept that relates the variation in length of the force produced by the components that make up the suspension to modify the vertical movement of the wheel.

Figure 1 shows the relative movement between the lower link and the coil-over/damper assembly which is calculated by equation 1.

$$MR = \frac{d1}{d2} \quad (1)$$

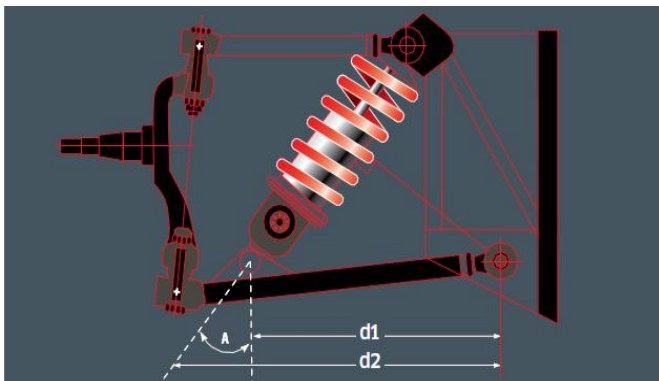


Fig. 1. Definition of the motion ratio. Source: [14]

Faced with a negative vertical displacement of the study suspension (descending), the extension phase of the shock absorber increases, causing the geometric index (MR) to change position and the wheel load index to decrease. If the trajectory described by the suspension is positive (ascending), the compression phase increases, the compression and therefore the extension or rebound decreases, which increases the wheel index and in turn causes the geometric index to change position, as shown in Figure 2. The design of the suspension control arms and the shock absorber stroke coincides with their maximum strokes; that is, the shock absorbers have a margin of 1 in. for both compression and extension. In this way the suspension geometry is not a constraint, but the limits are set by the shock absorbers.

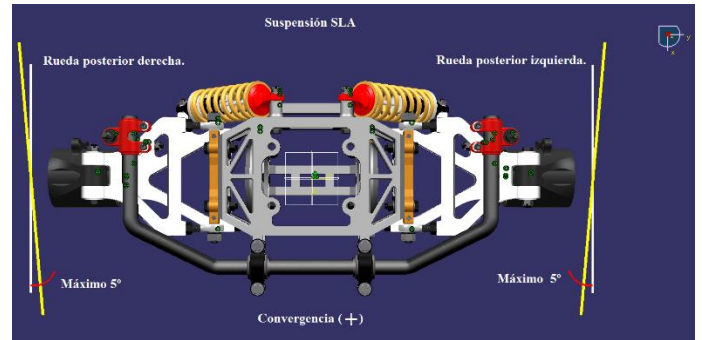


Fig. 2. Convergence and divergence

For the alignment of this parameter in the right section of the system it is required to disassemble only the upper control arm of the structural pivot and thus loosen the hexagonal lock nuts to rotate and align (insert) both ball joints in equal proportion to the desired position of camber angle (-) by moving the control arm into the system as shown in Figure 1, is a parameter that cannot be changed during a race and can only be adjusted in the workshop once the behavior of the car on the track has been felt. For each 0.25 in of displacement of the joints, the stub axle is positioned by 1°.

The alignment of this parameter in the left section of the system requires dismounting only the upper control arm from the structural pivot and thus loosening the hexagonal lock nuts in order to rotate and align (pull out) both ball joints in equal proportion to the desired camber angle position (+) as shown in Figure 3 by moving the control arm outward from the system, it is a parameter that cannot be changed during a stroke.

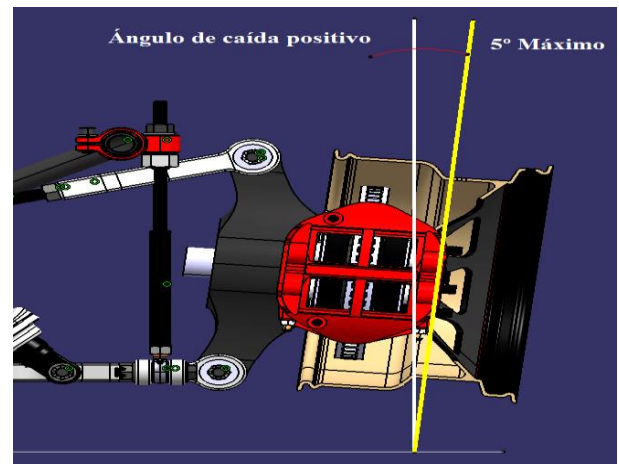


Fig. 3. Positive angle of repose

The correct placement of the drops is always set according to the tire reading after having driven a minimum of 5 or 6 laps on the circuit. Properly adjusted, they allow the car to tread well, allowing the tires to have homogeneous pressures, avoiding unequal pressure excesses in each part of each tire.

The loads on the wheels and the friction with the asphalt or concrete cause them to suffer more or less deformation depending on the position of the drops, affecting the effectiveness of grip. The more negative or positive they are, the more they hinder balance when driving. The more neutral, the more grip and control you have in a straight line, facilitating stability and grip when braking, but the position of the wheel is

not ready to turn, being 'narrower' for cornering. So you adjust the (positive or negative) drops (positive or negative) just and necessary.

When cornering, the support on negative camber orients the loads towards the chassis, which provides greater balance and grip when the tread is evenly distributed on the inclined plane of the camber. If they are too negative, the part furthest from the chassis on the outside wheels may not be used even during cornering, resulting in a lack of grip on the outside wheels, imbalance and uneven wear on each wheel.

3. RESULT

In this phase, the design of components is performed by knowing the behavior of the suspension components with the forces already calculated, in order to check whether the geometry of the parts is correct and whether or not they are capable of withstanding the racing conditions to which the system will be subjected. Once the preliminary results have been obtained through computational modeling, the geometry is optimized using the *Knowledgware Product Engineering Optimizer* module in order to adjust the geometry as best as possible and remove unnecessary material to lighten the part, but having as main criterion the integrity of the component without suffering permanent deformations that prevent a good use.

Factor of safety (F.S.). For the determination of the significant strength of the actual fabricated part and the details of the incident load, there is always some margin of uncertainty that must be covered by a factor of safety.

According to information provided by *Racecar Engineering* magazine, a safety factor between 2.5 and 3 is recommended for high-performance suspension systems.

Lower and upper control arms. These components are responsible for making the connection of the unsprung mass to the structural module that is assembled to the tubular chassis of the car, therefore, they are the critical parts of the entire assembly since they are responsible for modifying and transmitting the forces acting on the suspension system. The geometry of these components is as shown in Figure 4, the lower link has a length of 13 in long measured from the center of the connection strut to the connection points of the ball joints, while the upper control arm has a length of 9 in measured in the same way as in the lower link.

As one of the objectives proposed in the project is that the weight of the suspension design is lighter compared to the current system, it was thought to use aluminum alloys since its density is 1/3 that of steel, aluminum and its alloys are materials that stand out for their lightness and high strength.

The mechanical properties of pure aluminum are quite moderate, but when alloyed with other elements, they are significantly improved. When comparing specific strength or stiffness (in relation to density), aluminum is more advantageous than steel in certain applications in the aeronautical and automotive industries, among others.

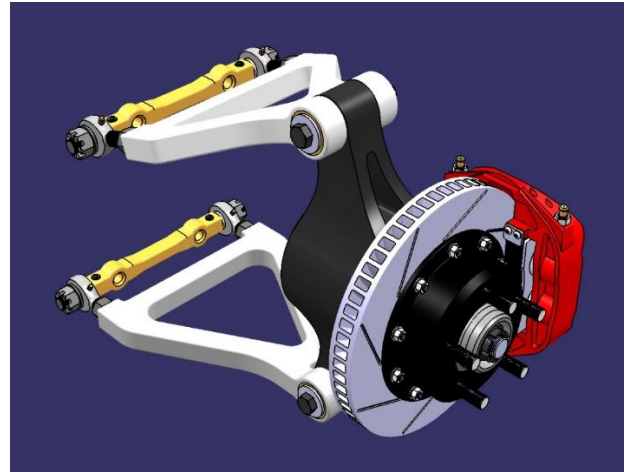


Fig. 4. Geometry of the control arms

For the calculation of stresses and finite element analysis, the aluminum casting alloy **355.0-T71** is used; Annex A contains the mechanical properties and chemical composition of this alloy. The important properties for the study are listed in Table 1.

Table 1. Mechanical properties of cast aluminum alloy **355.0-T71**

Mechanical properties	
Creep resistance (Sy)	27000 psi minimum
Compressive yield strength (Sxy)	31200 psi
Ultimate strength (Su)	34000 psi
Modulus of elasticity (E)	10300 Ksi
Shear strength (Sys)	26800 psi

Source: [15]

The design stresses to be worked with, given the magnitude of the calculated incident loads, are axial compressive and tensile stresses. For the definition of the design stresses, an S.F. equal to three is used, using equations 2, 3 and 4, from which the lowest value calculated is selected for the study.

$$\sigma_{\text{Diseño}} = \frac{S_{y,\text{Tesi3n}}}{F.S} \quad (2)$$

$$\sigma_{\text{Diseño}} = \frac{S_{y,\text{Compresi3n}}}{F.S} \quad (3)$$

$$\sigma_{\text{Diseño}} = \frac{S_u}{F.S} \quad (4)$$

According to the *Aluminum Association* (AA) the allowable or recommended bearing stress is given by equation 5.

$$\sigma_{\text{bd}} = 0.65 * Sy \quad (5)$$

The design stresses for creep resistance in both tension and compression for an S.F. of three for the components under study are as follows:

$$\text{Tensión} = \sigma_{\text{Diseño}} = \frac{S_{y,\text{Tensión}}}{\text{F.S}} = \frac{S_y}{3} = \frac{27000 \text{ psi}}{3} = 9000 \text{ psi}$$

$$\text{Compresión} = \sigma_{\text{Diseño}} = \frac{S_{y,\text{Compresión}}}{\text{F.S}} = \frac{S_y}{3} = \frac{31200 \text{ psi}}{3} = 10400 \text{ psi}$$

While the ultimate strength design stress and the allowable bearing stress are:

$$\sigma_{\text{Diseño}} = \frac{S_u}{\text{F.S}} = \frac{S_u}{3} = \frac{34000 \text{ psi}}{3} = 11333 \text{ psi}$$

$$\sigma_{\text{bd}} = 0.65 * 27000 \text{ psi} = 17550 \text{ psi}$$

The components of the right-hand section of the suspension system experience the greatest vertical load but this load is supported by the force elements such as the coil-over/shock absorber assembly and the stabilizer bar which must be designed to resist and oppose roll thus reducing lateral load transfer and making the car more parallel to the running surface.

When the car takes the curve at high speed it generates an equal and opposite inertia force called lateral force product of the centrifugal acceleration, therefore this force affects the right section as a compressive force while in the left section it affects as a tensile force. The maximum lateral load is experienced in the Bristol circuit since it is one of the fastest of the season, this force has a magnitude of 12727 lbf, but this must be uniform in each of the wheels, so on each section of the front and rear suspension systems affects a force of 3181.75 lbf.

Knowing the lateral load that affects the suspension system, the computational model is proposed only for the right section since it experiences the highest load, in order to simplify the study model by working with the maximum values to analyze the stress levels to which it will be subjected. Figure 5 below shows the results obtained for the lower right control arm.

To evaluate the cross-sectional geometry of the control arms, the axial forces incident on the control arms calculated in the static analysis are used.

$$\sigma_{\text{Cálculo}} = \frac{\text{F axial, Compresión y tensión}}{\text{Área sección transversal}} = \frac{2356.85 \text{ lbf}}{1.25 \text{ in} * 1.25 \text{ in}} = 1508.384 \text{ psi}$$

$$\sigma_{\text{Cálculo}} < \sigma_{\text{Diseño, Compresión}}$$

$$1508.384 \text{ psi} < 10400 \text{ psi}$$

$$\sigma_{\text{Cálculo}} < \sigma_{\text{Diseño, Tensión}}$$

$$1508.384 \text{ psi} < 9000 \text{ psi}$$

For the computational modeling of the component in Figure 5, a curvature based meshing was performed using tetrahedron type parabolic elements with a size of 0.125 in to obtain a mesh of excellent quality as shown in Table 2 of the meshing report in the pre-processing phase. The next step was to define the boundary conditions where fixed and user-defined embedment

constraints were used to simulate the assembly conditions of the system, as for the lateral load this was defined at the connection points of the control arm and the magueta, also the gravity acceleration (indicated with yellow vectors) and the lateral acceleration (indicated with white vectors) were taken into account.

According to the results obtained with the software, it is observed that the applied compressive force generates a maximum stress concentration value of 3870.964 psi at the connection point of the stabilizer bar guide arm.

The materials used in engineering can withstand enormous pressures (i.e. $\sigma_1 = \sigma_2 = \sigma_3 =$ high compression) without damage. Therefore, it is postulated that a given material has a limited and defined capacity to absorb distortion energy (i.e. energy that tends to change shape, but not size), and that subjecting the material to larger amounts of distortion energy causes creep. When using this theory it is convenient to work with an equivalent stress, σ_e , defined as the value of the uniaxial stress in tension that would produce the same level of distortion energy (therefore, according to the theory, the same possibility of failure) as the actual stresses indicated. In terms of the principal stresses that exist, Equation 6 is the expression for the equivalent stress.

$$\sigma_e = \frac{\sqrt{2}}{1} \cdot [(\sigma_2 - \sigma_1)^2 + (\sigma_3 - \sigma_1)^2 + (\sigma_3 - \sigma_2)^2]^{1/2} \quad (6)$$

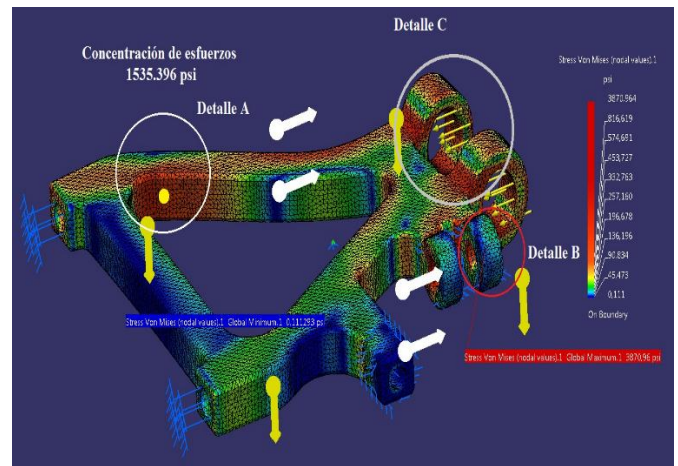


Fig. 5. FEM analysis for the lower control arm under compression

According to the calculations of the cross section, the axial compressive stresses have a magnitude of 1508.384 psi and in comparison to those calculated by the software they reach a value of 1535.396 psi, which is equivalent to a margin of error of 1.8% as shown in Figure 5 in detail A, the stress concentration appears on the internal face due to the variation of the geometry and is represented by the orange colored area. The other points in this section of the same color do not exceed the calculated compressive stress.

Table 2. Meshing report for the lower control arm

Meshing report				
	Entity	Size		
	Nodes	252794		
	Elements	159637		
Element type: Parabolic tetrahedron				
	Connectivity	Statistics		
	TE10	159637 (100,00%)		
Element quality				
Criteria	Excellent	Good	Mala	Average
Form	159637 (100,00%)	0 (0,00%)	0 (0,00%)	0,636
Appearance	156592 (98,09%)	3044 (1,80%)	1 (0,00%)	1,828

Source: [16]

In the section of the connection strut shown in Figure 6 in detail, there is a support stress due to the vertical load that it must support both in static and transient state, since it is a critical point because the mug holder is assembled by means of this strut. This point is now evaluated by calculating the support or crushing area due to the vertical load.

The projection of the support area is shown in Figure 6, where the geometry of the strut is observed to make the connection between the control arms and the stub axle by inserting a connecting pin in a hole of 1.5 in diameter as a fastening element. The projected area according to the geometry is

$$\text{Área proyectada} = 1.5 \text{ in} \cdot 1.125 \text{ in} = 1.875 \text{ in}^2$$

Having defined the geometry of the upper and lower control arm struts together with the incident radial load indicated in figure 6 with yellow arrows, the calculated stress is:

$$\sigma_{\text{Cálculdo}} = \frac{\text{Carga radial}/2}{\text{Área proyectada}} = \frac{2390.768 \text{ lbf}/2}{1.125 \text{ in} \cdot 1.5 \text{ in}} = 1195.384 \text{ psi}$$

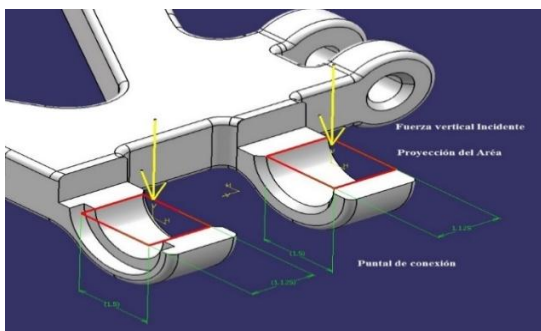


Fig. 6. Projection of the support area in the connection struts.

The comparison of efforts is:

$$\sigma_{\text{cálculdo}} < \sigma_{\text{recomendado}}$$

$$1195.384 \text{ psi} < 17550 \text{ psi}$$

As can be seen, the calculated working stress is below the recommended support stress, so the choice of F.S. of 3 is optimal given the magnitude of the loads being worked with, thus ensuring the integrity of the component. This result also applies to the upper control arm connection struts.

The lower control arm is now evaluated when the lateral force stresses the component (left control arm). Due to the stresses suffered in the element, it is observed that as in the case of the lateral force compressing the right control arm presents in the same location a maximum stress concentration with a magnitude of 1560.242 psi exceeding by 3.447 % the stress calculated for the cross section.

Figure 7 shows the graphical results of the stress plot analysis under the Von Mises criterion. The stress concentration is highlighted by detail A, in this section of the component the stress concentration is due to the change in the cross-section geometry and is represented by the orange colored area. The other orange colored points are below the design stress. The stress concentration detected in both cases is not severe enough to cause permanent deformation in the component, therefore it is not necessary to modify the cross-sectional area.

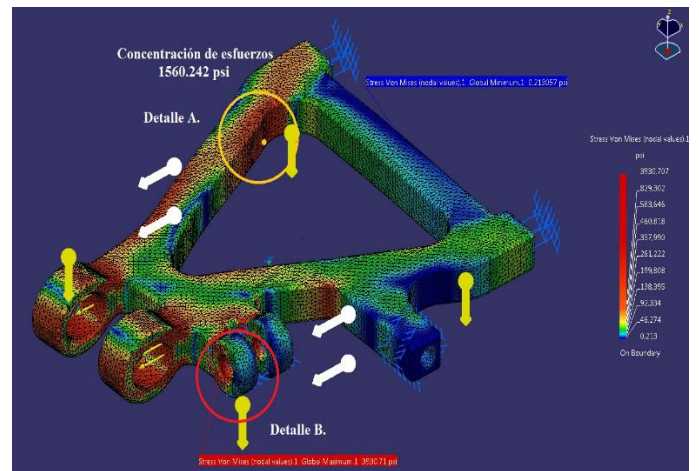


Fig. 7. FEM analysis for the lower control arm under compression

The analysis of the upper control arms is also performed both in compression and tension according to the incident lateral force. For the evaluation of the cross-section geometry, the axial forces are calculated with the calculated internal forces resulting from the lateral force. The calculation of the respective forces is:

$$\sigma_{\text{Cálculdo}} = \frac{\text{Faxial, Compresión}}{\text{Área transversal}} = \frac{1667.62 \text{ lbf}}{1.25 \text{ in} \cdot 1.25 \text{ in}} = -1067.27 \text{ psi}$$

$$\sigma_{\text{Cálculdo}} < \sigma_{\text{Diseño, Compresión}}$$

$$1067.27 \text{ psi} < 10400 \text{ psi}$$

$$\sigma_{\text{Cálculo}} = \frac{\text{F axial, Tensión}}{\text{Área transversal}} = \frac{1667.62 \text{ lbf}}{1.25 \text{ in} \cdot 1.25 \text{ in}} = 1067.27 \text{ psi}$$

$$\sigma_{\text{Cálculo}} < \sigma_{\text{Diseño, Tensión}}$$

$$1067.27 \text{ psi} < 9000 \text{ psi}$$

Figure 8 shows the graphic results of the stress plot analysis under the Von Mises criterion. A stress concentration is observed in the internal faces of the section in the zones showing details B, this is due to the variation of the geometry of the cross section, the maximum value reached by this stress concentration has a magnitude of 4962.85 psi when the element is subjected to compression, while in the case where it is subjected to tension it reaches a maximum value of 4864.6 psi, these values are presented in both internal faces of the component because they are symmetrical for both cases. Another point of slight stress concentration is the zone shown by details C, in this section there is variation of the geometry and the values that are reached when the lateral force impacts and compresses the component have a magnitude of 1679.431 psi and for the opposite case, that is, in tension, the stress concentration reaches a maximum value of 1848.326 psi. In the sections where the geometry is constant (a área transversal $1.25 \text{ in} \cdot 1.25 \text{ in} = 1.5625 \text{ in}^2$) a value of 1067.768 psi is reached both in tension and compression, which corresponds to the value calculated with an error margin of 0.045%. It can be observed that the maximum stresses are located at the points described above, this result is logical taking into account that the sections are perpendicular to the stress and that one of their ends is very close to the points where the spherical plain bearings are secured, which have been immobilized for the analysis. The stress concentration is dispensable since the values calculated in the software are below the design stresses so there is no need to change the geometry of the control arm.

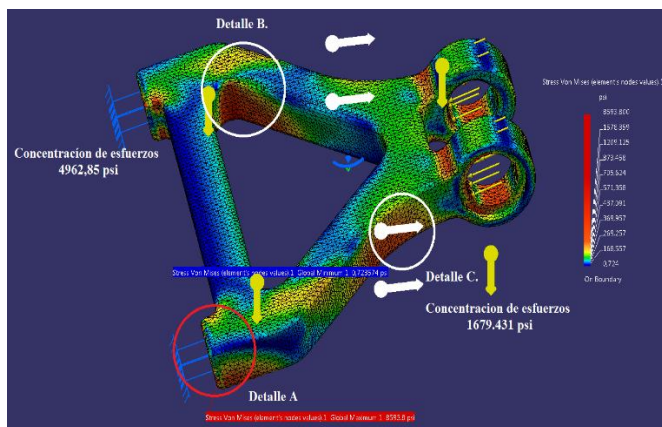


Fig. 8. FEM analysis for the upper control arm.

Structural connecting pin. This component allows the connection between the struts of the control arms, thus allowing to support the shear product of the load on the right rear wheel due to the longitudinal and transverse transfer, acceleration, deceleration and G forces to which it is subjected. The same steel used to build the stabilizer bars is used for this component,

as it is a connecting element. The mechanical properties are included in Annex A and the properties required for the calculations are listed in Table 3 below.

Table 3. Mechanical Properties of UNS H43400 Steel

Mechanical properties	
Creep resistance (Sy)	284900 psi
Ultimate strength (Su)	269900 psi
Shear strength (Sys)	101500 psi
Young's modulus (E)	29700 Ksi
Modulus of rigidity (G)	11600 Ksi
Poisson's ratio	0.290

Source: [15]

Since there is no calculated value available for the shear creep resistance of the material S_{ys} we resort to the AISC estimate which is equal to half of the ultimate strength. The loads to evaluate the integrity of the component are the vertical force on the connection strut of 1784.5865 lbf and the lateral load with a value of 1590.875 lbf calculated in the static analysis of the right section of the suspension system, which is where the highest loads occur, together with the maximum lateral acceleration, which has a magnitude of 3.6889 G's

The estimate for shear strength is given by equation 6.

$$S_{ys} = \frac{S_u}{2} \tag{6}$$

$$S_{ys} = \frac{269900 \text{ psi}}{2} = 134.95 \text{ Ksi}$$

Thus, the calculated shear design stress is:

$$\tau_{\text{Diseño}} = \frac{S_{ys}}{F.S} = \frac{134.95 \text{ Ksi}}{3} = 44.983 \text{ Ksi}$$

A 5/8"-18 UNF-3A- 5.5" SAE 1 GRADE bolt is used to fasten the element, the cross-sectional area for the geometry of the component is:

$$\text{Área de la geometría} = \frac{\pi}{4} ((1.5")^2 - (5/8" + 1/16")^2)$$

$$= 1.395922517 \text{ in}^2 \sim 1.5 \text{ in}^2$$

$$\tau_{\text{Cálculo}} = \frac{2390.768 \text{ lbf}/2}{1.5 \text{ in}^2} = 797 \text{ psi}$$

$$\tau_{\text{Cálculo}} < \tau_{\text{Diseño}}$$

$$797 \text{ psi} < 44.983 \text{ Ksi}$$

The discretization of the model was performed by means of a meshing based on shape or curvature, which allows a much better control of the meshing on edges and curved faces. As for the element size, a value of 0.125 in was taken to have an excellent or good quality mesh in order to have the best possible accuracy in the results. The boundary conditions used were fixed embedment for the external connection faces.

4. CONCLUSION

This article proposes the design of components with Catia software of the suspension of competition vehicles, performing a 3D simulation, with which you can determine in advance the best model to manufacture that meets the specifics of the parts that have the suspension, that is why the design will result in savings in manufacturing time, as well as in the increase of measures according to the parameters established for each of the components, presenting the process for the numerical calculation to be implemented in the modeling software.

REFERENCES

- [1] V. L. R. Rivero, «Evolución del uso de los materiales plásticos en la industria automotriz», *INNOVA Res. J.*, vol. 3, n.º 12, Art. n.º 12, dic. 2018, doi: 10.33890/innova.v3.n12.2018.928.
- [2] «Materiales reforzados que marcan tendencia en automotriz». <https://www.pt-mexico.com/articulos/materiales-reforzados-que-marcan-tendencia-en-automotriz> (accedido ago. 03, 2021).
- [3] J. L. Valentin *et al.*, «Diseño y desarrollo sostenible de materiales poliméricos», *Rev. Plast. Mod.*, vol. 115, p. 19, ene. 2018.
- [4] D. Vertus, J. Henríquez, y M. Ruiz, «Biodegradación bacteriana de polietileno y propuesta de aplicación para Cerro Patacón», jun. 2017.
- [5] M. C. Arela, F. S. Masco, R. A. C. Churac, J. E. V. Rivera, y J. C. Calla, «Biodegradación de polímeros de plástico por *Pseudomonas*», *Rev. Investig. Cienc. Tecnol. Desarro.*, vol. 6, n.º 2, Art. n.º 2, 2020, doi: 10.17162/rictd.v6i2.1457.
- [6] «Autobody Magazine | La fibra de carbono en las carrocerías modernas». <https://www.autobodymagazine.com.mx/2018/02/01/la-fibra-de-carbono1/> (accedido ago. 03, 2021).
- [7] «La fibra de carbono, de la pista de carreras a la carretera», *BBC News Mundo*, mar. 10, 2011. https://www.bbc.com/mundo/noticias/2011/03/110310_uto_fibra_carbono_pl (accedido ago. 03, 2021).
- [8] M. M. Theurer, J. Rodriguez, Alcívar, López, Soriano, y Villacis, «Las fibras de carbono como una alternativa para reforzamiento de estructuras», *Ingeniería*, vol. 20, n.º 1, pp. 57-62, 2016.
- [9] B. Kedar, B. Ashok, N. Rastogi, y S. Shetty, «Design and analysis of automobile components using industrial procedures», *IOP Conf. Ser. Mater. Sci. Eng.*, vol. 263, p. 062035, nov. 2017, doi: 10.1088/1757-899X/263/6/062035.
- [10] S. S. Sharma Roopesh Tiwari, Suman, «Design and Analysis of Heavy Commercial Vehicle Chassis Through Material Optimization», *Int. J. Eng. Trends Technol. - IJETT*, Accedido: ago. 03, 2021. [En línea]. Disponible en: <https://ijettjournal.org/archive/ijett-v67i12p205>
- [11] V. S. N, «Effect of Cross-Sections Considering Material and Design Aspects in Automotive Chassis», Accedido: ago. 03, 2021. [En línea]. Disponible en: https://www.academia.edu/16194658/Effect_of_Cross_Sections_Considering_Material_and_Design_Aspects_in_Automotive_Chassis
- [12] «Design and ANSYS analysis of Components of Wheel Assembly of SAE Car - Inpressco». <https://inpressco.com/design-and-ansys-analysis-of-components-of-wheel-assembly-of-sae-car/> (accedido ago. 03, 2021).
- [13] E. Olmos, «15 preguntas que siempre quisiste hacer sobre NASCAR», *Atracción360*, feb. 14, 2017. <https://www.atraccion360.com/como-entender-la-nascar> (accedido ago. 03, 2021).
- [14] «Eibach: Suspension Replacement». <https://www.eibach.de/en/chassis/suspension-replacement> (accedido ago. 03, 2021).
- [15] «Online Materials Information Resource - MatWeb». <http://www.matweb.com/> (accedido ago. 03, 2021).
- [16] «CATIA V5 Student Edition | 3DEXPERIENCE Edu». <https://academy.3ds.com/en/software/catia-v5-student-edition> (accedido ago. 03, 2021).